A Flow Field Guided Path Planning Method for Unmanned Ground Vehicle

Nan Wang[1], Mengxuan Song[1], Jun Wang[1*], Timothy Gordon[2]

***Abstract*—This paper focuses on the path planning problem for Unmanned Ground Vehicles(UGVs) in complex environment. Fluid flow is applied to the path planning method for the outstanding performance in finding the outlet. The proposed method consists of two layers–the flow field layer and the optimization layer. The flow field layer provides a velocity distribution which describes the fluid flowing from a starting point to a terminal point. The solution of the flow field is obtained by Computational Fluid Dynamics(CFD) method. The optimization layer generates a specific path and guarantees the manoeuvrability of the path. The proposed method is tested in several scenarios, through which its good performance is well demonstrated.**

I. INTRODUCTION

In recent years, the path planning problem for UGVs has attracted much attention. The reference path influences the performance of the control module significantly. One of the key challenges in path planning is generating a smooth path in complex environment considering non-holonomic constraints.

Various path planning methods have been developed. Conventional graph search algorithms, such as Dijkstra algorithm [1], A* algorithm [2] and D* algorithm [3], search the global map for a path. But graph search algorithms are designed only for holonomic systems and not appropriate for UGV application.

Artificial intelligent(AI) algorithms have been successfully implemented in path planning including fuzzy logic algorithm [4], genetic algorithm [5] and neural networks algorithm [6]. AI based planning algorithms can handle vehicle kinematics constraints and environment constraints, but solutions are not always available. Similar methods such as model based optimization algorithm [7] are also proposed, which share the same drawbacks.

Much efforts have been devoted to sampling based planners such as Rapidly-exploring the Randomized Tree (RRT) [8] and the Probabilistic Road Map (PRM) [9]. One key drawback of the sampling-based path planning method is that the probabilistic completeness is achieved only when the number of samples approaches infinity. Also, they are not appropriate for non-holonomic systems.

Artificial Potential Field (APF) method is another conventional method for path planning [10]. APF method provides a smooth and collision-free path. But there are local minima in the potential field, which makes it inappropriate for path planning in complex environment [11]. Basically the traditional APF method consists of two steps. The first is to define a potential field function and the second is to simulate a particle moving according to the potential field. Several improved APF methods were proposed to deal with the drawbacks but most of them focused on the folloing process [12]. The rest tried to modify the definition of potential field. Reference [13] proposed a rotational potential field to avoid being stuck in local minima by making the repulsive force tangent to the potential field. Nevertheless, only the case with a single convex obstacle is considered and the feasibility in complex scenarios remains unconfirmed. Besides, Reference [14] proposed a harmonic potential field(HPF) to guide the particle. In HPF, no local minima exist even when there are multiple convex obstacles. But all the obstacles have to be expanded to spheroids, which wastes free space. Therefore the problems are rendered unsolvable in narrow space.

Different from all the methods listed above, a novel and effective path planning method is proposed innovated by fluid flow. Fluid flow has many properties that can be used to provide the guidance. First, according to the law of conservation of mass, if incompressible fluid flows into an inlet, fluid will always flow out of the outlet. Second, it is demonstrated that fluid always moves along a collision-free path. Third, flow field is smooth.

The overall structure of the proposed method consists of two layers. In the top layer, a flow field within free space is obtained by CFD using ANSYS software package. In the bottom layer, an optimization method is developed to find a feasible path. In this paper, vehicle model is used in three aspects: 1) analysis of vehicle body's velocity distribution; 2) update of vehicle states; 3)model constraints in optimization process. As an essential component in the optimization layer, the cost function consists of two parts. One is to guide a simulated vehicle following the fluid flow. The other is to avoid collisions. The optimization problem is solved in receding manner. The steering angle is obtained at each step. A specific path is calculated based on the steering angle sequence.

The paper is structured as follows: Section II describes the hypothesis, governing equations and boundary conditions in the flow field layer. Section III presents details about the optimization layer including the vehicle model, the cost function and the optimization process. In Section IV, results are given to demonstrate the performance of the proposed method. Finally, Section V summarizes the contributions of the paper and maps out future research directions.

This work was supported by the National Natural Science Foundation of China (NSFC) under Grant No. 61473209.

[1]Nan Wang, Mengxuan Song and Jun Wang are with the Department of Control Science and Engineering, Tongji University, Shanghai 201804, P.R.China.

[2]Timothy Gordon is with the School of Engineering, University of Lincoln, Lincoln, Lincolnshire, United Kingdom

*Corresponding author: junwang@tongji.edu.cn

II. Flow Field Layer

One of the most novel parts of this paper is using the fluid flow as guidance. In this section, a brief description about CFD is presented.

A. Hypothesis

Since the CFD is introduced not to simulate a realistic fluid phenomenon, but to provide a reference for path planning, the fluid matter is merely imaginary, and several hypothesis and simplifications should be made during the generation of the flow field. (1) Due to the requirement of smoothness of the path, flow field with turbulence would not make a good candidate. Therefore the flow field is purely laminar, and its Reynolds number would be sufficiently low. (2) In order to obtain consistent path planning strategy for all possible circumstances, boundary conditions during the solving of the flow field should not be intervened by any case-specific adjustments, but determined by the starting point, the target point and the obstacles only. (3) The discretized mesh of the computational domain does not need to be refined to resolve boundary layers, and in the mean time, it must be fine enough to provide smooth interpolations for the vehicle movement.

Although other properties of the fluid remain uncertain, some simplified settings are used, for that our concern is whether the flow field can provide a good reference for path planning rather than resolve real physical phenomenon. (1) Physical properties of the fluid are constant. (2) The fluid is incompressible. (3) The gravitational force is not considered.

B. Governing equations

With the hypothesis and simplification described above, the governing equations of the fluid flow are the continuum equation and the momentum conservation equations, as listed below.

$$\nabla \mathbf{u} = 0 \tag{1}$$

$$\rho \mathbf{u} \cdot \nabla \mathbf{u} = -\nabla p + \nabla \cdot (\mu \nabla \mathbf{u}), \tag{2}$$

where $\mathbf{u}$ is the velocity vector, ρ is the fluid density, μ is the molecular viscosity. In the present study, the values are chosen according to the air under normal state.

C. Boundary conditions

The boundary conditions during the solving of the flow field are set as follows. (1) The wall behind the vehicle at the starting point has uniform velocities at a fixed value (10^{-5}m/s in the present study), with directions perpendicular to the wall and pointing into the domain. (2) The wall in front of the vehicle at the terminal point is set as a fully developed outlet. (3) Other walls are no-slip solid borders.

D. CFD Simulation

1) Mesh generation: A mesh has to be generated to discretize the calculation domain. ANASYS ICEM CFD 15.0 is employed to achieve the aim. The density of the nodes has to guarantee that the vehicle body covers moderate number of nodes. If the vehicle body covers too few nodes, the generated path will be unsmooth. If the vehicle body covers too many nodes, the burden of computation will be unnecessarily increased.

Taking an 80m$\times$ 60m map as an instance, as is shown in Figure 1, 55926 nodes are generated. Considering a normal vehicle with length of 4.5m and width of 1.8m, vehicle body occupies about 94.38 nodes on average.

2) fluid flow calculation: ANSYS Fluent is a professional CFD software to calculate the velocity distribution in the flow field.

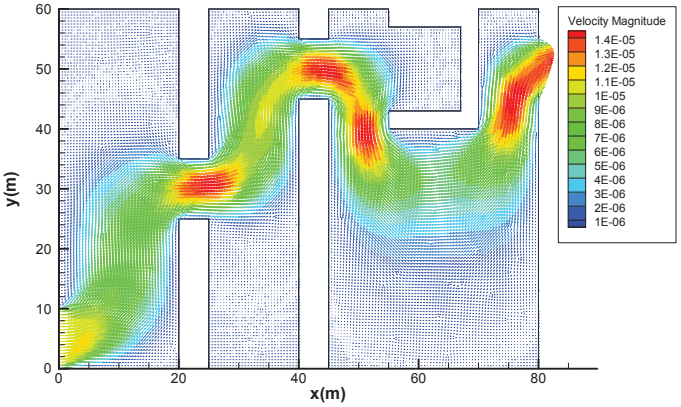

Fig. 1. Flow field in Scenario 1

III. Optimization Layer

Optimization layer is to search the fluid flow field for a feasible path. Three key elements must be taken into account: (1) non-holonomic velocity constraints, (2) rigidity of the vehicle and (3) collision avoidance. The first element is formulated as a specific constraint by employing the vehicle model. The element (2) and (3) are modelled as two parts of the cost function. By solving the optimization problem in receding manner, the path is obtained.

A. Vehicle model

The vehicle model is shown in Figure 2. Manoeuvres are assumed to have zero sideslip angles because only low speed condition is considered. The state of the model is $[x, y, \theta]^\top$, where x and y are the coordinates of the middle point of the rear axle in a global coordinate system and θ is the heading angle of the vehicle body with respect to the x axis. v is longitude velocity and δ is the steering angle of the front wheels which can be taken as input. l is the distance between the front and rear axles. The vehicle model is:

$$\begin{cases} \dot{x} = v\cos\theta \\ \dot{y} = v\sin\theta \\ \dot{\theta} = v\frac{\tan\delta}{l}, \end{cases} \tag{3}$$

where $|\delta| \leq \delta_{max}$.

Assuming that the longitude velocity is constant and time domain is discretized, the state $X(t+1)$ in the next step can

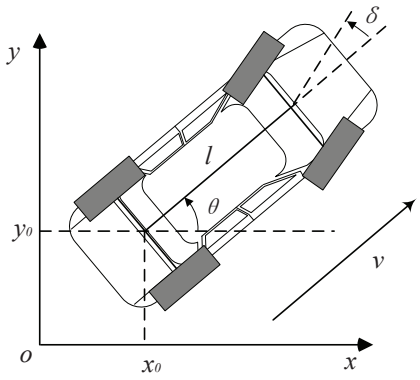

Fig. 2. Vehicle model

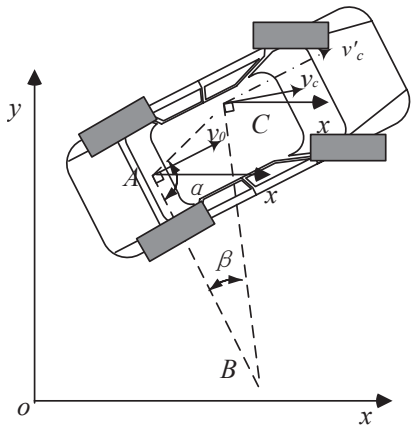

Fig. 3. Geometric deduction to calculate velocity distribution of vehicle body

be calculated based on current state $X(t)$ and input $\delta(t)$. If steering turns to the left side, $\delta(t) > 0$:

$$\begin{cases} d = v \times 1 \\ x(t+1) = x(t) + d \times \cos\theta(t) \\ y(t+1) = y(t) + d \times \sin\theta(t) \\ \theta(t+1) = \theta(t) + d \times \frac{\tan\delta(t)}{l}. \end{cases} \tag{4}$$

B. Cost function

A feasible reference path is generated by minimizing the cost function in receding manner. the cost function includes the element of coherence with the flow field and the element of collision alarms.

1) Coherence with the fluid flow: Flow field represents the underlying guidance for goal seeking. Consequently the disparity between the velocity distribution of the vehicle body and that of the fluid flow should be minimized. The velocity distribution of the vehicle body is calculated under the input δ according to geometric deduction and the vehicle model. Mean value of the disparity of all the nodes represents the coherent level.

The front left part of the vehicle body is taken as an example. As is shown in Figure 3, Point A is the middle point of the rear axle. According to the vehicle model, the trajectory approximates an arc. Point B is the center of the circle when the steering angle equals δ. Point C represents one of the points within the vehicle body. The coordinates of Point A and C are known as (x_a, y_a) and (x_c, y_c). The length of AB is obtained from input δ based on the vehicle model.

$$AB = \frac{l}{\tan(\delta)}. \tag{5}$$

The geometric deduction is detailed as follows. $< \cdot, \cdot >$ means the absolute value of included angle between two vectors. $\vec{e_x}$ represents unit vector in the direction of x axis.

$$\begin{cases} AC = \sqrt{(x_a - x_c)^2 + (y_a - y_c)^2} \\ \angle\alpha = \arctan(\frac{y_c - y_a}{x_c - x_a}) - < \vec{v_0}, \vec{e_x} > + \frac{\pi}{2}. \end{cases} \tag{6}$$

According to Cosine Law,

$$\begin{cases} BC = \sqrt{AB^2 + AC^2 - 2 \times AB \times AC \times \cos\angle\alpha} \\ \angle\beta = \arccos\frac{AB^2 + BC^2 - AC^2}{2 \times AB \times BC} \\ < \vec{v_0}, \vec{v_c} > = \angle\beta. \end{cases} \tag{7}$$

The direction of $\vec{v_0}$ equals that of the heading since the sideslip is ignored in the present study. Therefore the direction of $\vec{v_c}$ is obtained:

$$< \vec{v_c}, \vec{e_x} > = < \vec{v_0}, \vec{e_x} > - < \vec{v_0}, \vec{v_c} >, \tag{8}$$

where $\vec{v_c}$ is the velocity of vehicle body at point C. $\vec{v_c}'$ is the velocity of the fluid flow at point C. $< \vec{v_c}, \vec{v_c}' >$ is chosen to describe the disparity at point C. Ω_t represents the point set within the vehicle body at state $X(t)$. As is shown in Figure 4, mean value of the disparity of all the nodes within Ω_t represents the disparity between the vehicle and the flow. N_t represents the number of nodes within vehicle body at state $X(t)$. Cost function in terms of coherence is defined as:

$$F_c = \frac{1}{N_t} \sum_{C \in \Omega_t} < \vec{v_c}, \vec{v_c}' > . \tag{9}$$

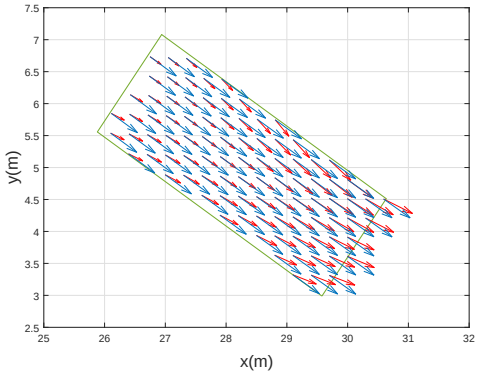

Fig. 4. Coherence between velocity distribution of the vehicle body and that of the flow field. Blue arrows represent the velocity distribution of the fluid flow and red arrows represent that of the vehicle body.

TABLE I
PARAMETERS TABLE

Parameter Name	Value	Units
Length	4.50	m
Width	1.855	m
Wheelbase	2.65	m
δmin	-28.18	deg
δmax	28.18	deg
Penalty Value	10000	-

2) Alarm of the collision: Collisions equal the situation that vehicle body and the obstacle have overlap. F_a is added if the overlap is detected in the next step. The penalty value is set as a relatively large value. It has been proven that results are not sensitive to the penalty value.

$$F_a = \begin{cases} 0 & \text{if collision isn't detected} \\ \text{PENALTY\_VALUE} & \text{if collision is detected.} \end{cases} \quad (10)$$

C. Optimization Problem

To obtain a feasible reference path without collisions, the following problem is solved at each step.

The cost function is

$$\min_{\delta} F = F_c + F_a. \quad (11)$$

The velocity distribution of vehicle body is calculated by (5)-(8) while velocity distribution of fluid flow is obtained by (1)-(2). Equation (9) is used to describe the disparity between both of them. The constraint of input is:

$$|\delta| \leq \delta_{max}. \quad (12)$$

Interior-point method is used to solve the minimization problems in the real-number domain. The optimization problems are implemented by the function *fmincon* in Matlab Optimization Toolbox. According to the solution δ and velocity v, the state of vehicle is updated by function (4). The iteration will not stop until the distance between the current position and the terminal position is less than a threshold.

IV. SIMULATION AND RESULTS

The performance of the proposed double-layer path planning method is verified in typical scenarios. Details about the simulation and results are described in this section.

A. Simulation Setup

The searching method is implemented in MATLAB on the IBM BladeCenter HS22 servers. As Table I shows, some important parameters used to describe the vehicle model are derived from an MGGS 1.6T experiment vehicle in our lab.

B. Simulation Results

There are six scenarios designed in the simulation:

- A complex maze.
- Merging while avoiding obstacles.
- U-turn.
- Turning left at an intersection.
- Leaving a parking lot.
- Leaving a warehouse.

The first scenario is to demonstrate that the proposed method is able to generate a path in a complex map with a concave obstacle. The second scenario is to confirm that the path is relatively smooth. The Scenario 2 describes merging while avoiding obstacles. The rest four scenarios are designed to simulate some practical situation.

The flow field in Scenario 1 is shown in Figure 1. Figure 5 presents the result of the proposed method. The purple curve is the path, which avoids the collision and reaches the terminal point smoothly. There is no local minima in fluid flow where path generated by other methods like APF may get trapped.

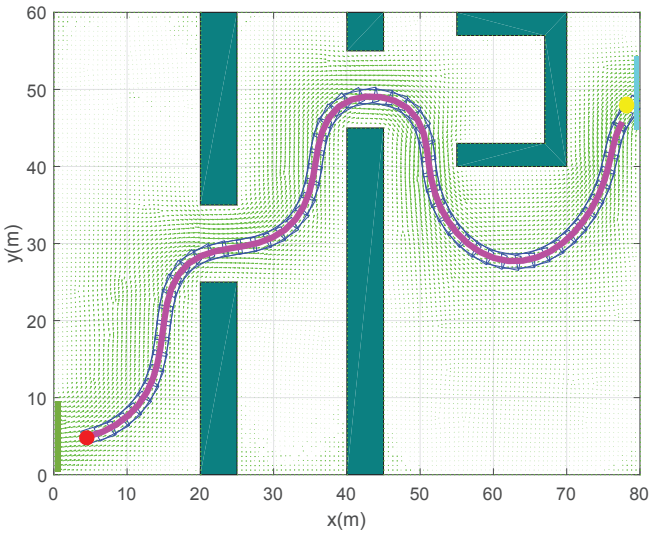

Fig. 5. Path planning result in Scenario 1. Dark green rectangles represent the obstacles. Red dot represents starting point and yellow dot represents the terminal point. The green rectangle represents the inlet and the light blue rectangle represents the outlet. Light green arrows represent the velocity distribution of flow field. The dark blue lines represent the vehicle body at each frame. Purple curve represents the path generated using the proposed method. That no overlap exists between the obstacles and the vehicle proves the path is collision-free.

As is shown in Figure 6(a) and 6(b), the front wheel steering angles and the heading angles during the simulation are recorded. The steering angles during the simulation are within the range of $[-\delta_{max}, \delta_{max}]$. The curve of heading angles in the experiment is smooth.

Scenario 2 is presented to simulate the situation when car merges into an adjacent lane while avoiding the obstacles. Figure 7, 8 and 9 show the flow field, result and performance in scenario 2 respectively.

The length of the path is used to evaluate the efficiency. Under the assumption that the longitude velocity of the vehicle is constant, the heading angle can not change sharply for the smoothness requirement. The mean value and standard deviation of absolute angular velocity represent the variation trend of heading angle. The maximum of the absolute angular velocity represents the sharpest change of heading angle. All

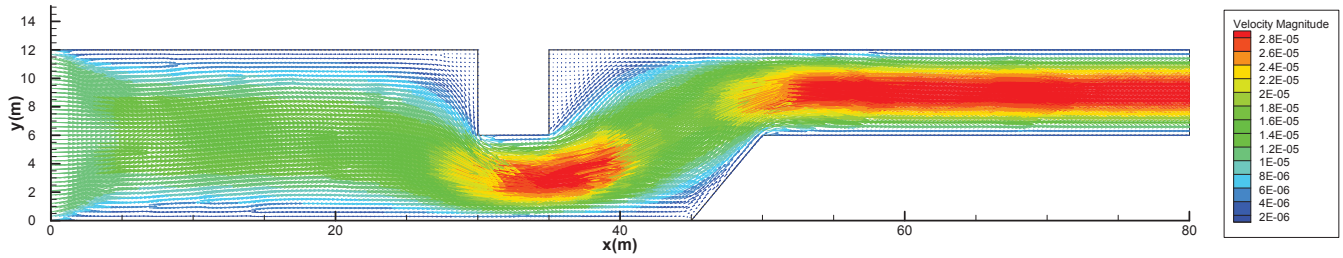

Fig. 7. Flow field in Scenario 2

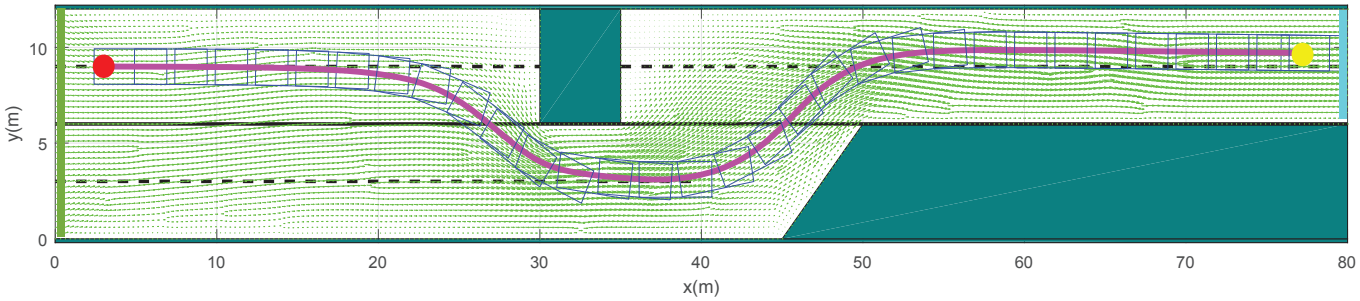

Fig. 8. Result of Scenario 2

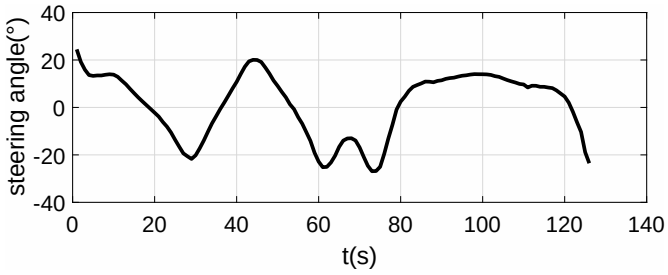

(a) Front Wheel Steering Angle

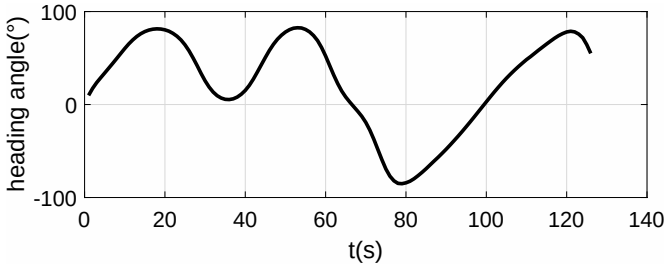

(b) Heading Angle

Fig. 6. Performance of the proposed method in Scenario 1

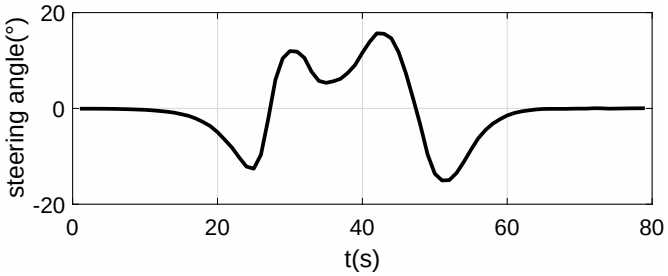

(a) Front Wheel Steering Angle

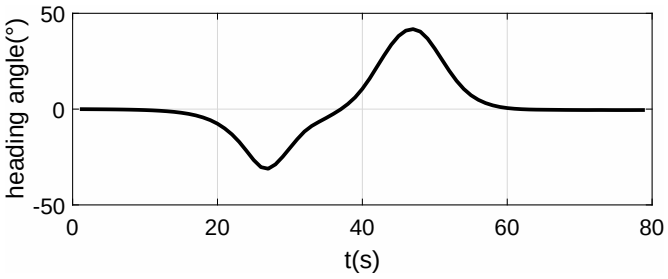

(b) Heading Angle

Fig. 9. Performance of proposed method in Scenario 2

of the three metrics are essential to quantify the smoothness of the path.

The rest of the results are as Figure 10 shows. The proposed method is proven to be applicable to various scenarios. Particularly, result in scenario 10(c) proves that the method also works in limited free space. The longitude velocity in scenario 10(c) is set relatively low for its higher requirement for precision of operation. Table II shows the performance in all the scenarios. As is shown in the Table II, the mean value, standard deviation and maximum of angular velocity in all the scenarios are at low level, which proves its smoothness.

V. CONCLUSIONS

In this paper, a path planning method is designed for UGV by utilizing the properties of the fluid flow. The main advantage of the algorithm is the ability to solve complex geometric problems and to generate smooth and collision-free

TABLE II
PERFORMANCE IN EACH SCENARIOS

Scenario No	Longitude velocity	Length	Mean value of absolute angular velocity	Standard deviation of absolute angular velocity	Maximum of absolute angular velocity
1	1m/s	125m	4.6424 deg/s	2.5251 deg/s	10.961 deg/s
2	1m/s	78m	1.8755 deg/s	2.0028 deg/s	6.0688 deg/s
3	1m/s	25m	7.2210 deg/s	4.7304 deg/s	11.588 deg/s
4	1m/s	26m	3.4545 deg/s	3.0603 deg/s	7.2215 deg/s
5	0.2m/s	22m	0.81863 deg/s	0.85534 deg/s	2.3176 deg/s
6	1m/s	107m	1.6816 deg/s	1.9596 deg/s	7.6832 deg/s

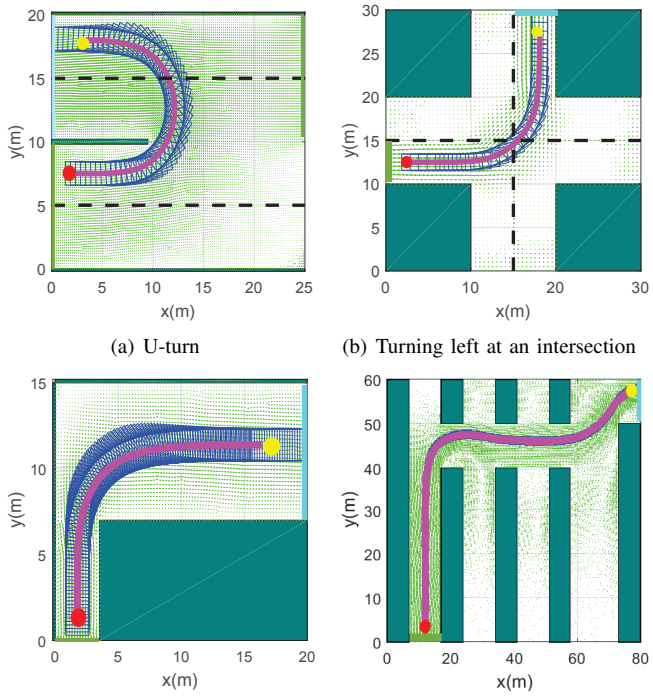

(a) U-turn (b) Turning left at an intersection

(c) Leaving a parking lot (d) Leaving a warehouse

Fig. 10. Results of the remaining four scenarios

path for non-holonomic systems. It is the first time that fluid flow field is applied to path planning method.

As the proposed method is novel, there are still some problems to be solved. First, if the fluid flow is divided into two branches and the flux of both is approximately the same, the solution of the optimization problem may lead to collision. Besides, we are going to design the intelligent setting of the inlet and outlet of fluid flow. Finally, it is still a challenge to deal with dynamic environment with uncertainties. We will devote more efforts to environment modelling in the future.

REFERENCES

[1] E. W. Dijkstra, "A note on two problems in connexion with graphs," *Numerische Mathematik*, vol. 1, no. 1, pp. 269–271, 1959.

[2] A. Stentz, "Optimal and efficient path planning for partially-known environments," in *IEEE International Conference on Robotics and Automation*, 1994, pp. 3310–3317.

[3] M. Likhachev, D. I. Ferguson, G. J. Gordon, A. Stentz, and S. Thrun, "Anytime dynamic a*: An anytime, replanning algorithm," in *The International Conference on Automated Planning and Scheduling (ICAPS)*, 2005, pp. 262–271.

[4] A. Saffiotti, "The uses of fuzzy logic in autonomous robot navigation," *Soft Computing*, vol. 1, no. 4, pp. 180–197, 1997.

[5] K. H. Sedighi, K. Ashenayi, T. W. Manikas, R. L. Wainwright, and H.-M. Tai, "Autonomous local path planning for a mobile robot using a genetic algorithm," in *Evolutionary Computation*, vol. 2, 2004, pp. 1338–1345.

[6] M. J. Phinni, A. Sudheer, M. RamaKrishna, and K. Jemshid, "Obstacle avoidance of a wheeled mobile robot: A genetic-neurofuzzy approach," in *IISc Centenary-International Conference on Advances in Mechanical Engineering*, 2008.

[7] C. Li, J. Wang, X. Wang, and Y. Zhang, "A model based path planning algorithm for self-driving cars in dynamic environment," in *Chinese Automation Congress*, 2015, pp. 1123–1128.

[8] S. M. LaValle and J. James J. Kuffner, "Randomized kinodynamic planning," *The International Journal of Robotics Research*, vol. 20, no. 5, pp. 378–400, 2001.

[9] L. E. Kavraki, P. Svestka, J. C. Latombe, and M. H. Overmars, "Probabilistic roadmaps for path planning in high-dimensional configuration spaces," *IEEE Transactions on Robotics and Automation*, vol. 12, no. 4, pp. 566–580, 1996.

[10] O. Khatib, "Real-time obstacle avoidance for manipulators and mobile robots," in *Autonomous robot vehicles*, 1986, pp. 396–404.

[11] G. Li, S. Tong, G. Lv, R. Xiao, F. Cong, Z. Tong, A. Yamashita, and H. Asama, "An improved artificial potential field-based simultaneous forward search (improved apf-based sifors) method for robot path planning," in *12th International Conference on Ubiquitous Robots and Ambient Intelligence*, 2015, pp. 330–335.

[12] M.-H. Kim, J.-H. Heo, Y. Wei, and M.-C. Lee, "A path planning algorithm using artificial potential field based on probability map," in *2011 8th International Conference on Ubiquitous Robots and Ambient Intelligence*, 2011, pp. 41–43.

[13] H. Rezaee and F. Abdollahi, "Adaptive artificial potential field approach for obstacle avoidance of unmanned aircrafts," in *IEEE/ASME International Conference on Advanced Intelligent Mechatronics (AIM)*, 2012, pp. 1–6.

[14] D. Lau, J. Eden, and D. Oetomo, "Fluid motion planner for nonholonomic 3-d mobile robots with kinematic constraints," *IEEE Transactions on Robotics*, vol. 31, no. 6, pp. 1537–1547, 2015.